Ezrin Promotes Morphogenesis of Apical Microvilli and Basal Infoldings in Retinal Pigment Epithelium

Vera Lúcia Bonilha,* Silvia C. Finnemann,*‡ and Enrique Rodriguez-Boulan*‡

*Margaret M. Dyson Vision Research Institute, Department of Ophthalmology, and ‡Department of Cell Biology, Weill Medical College of Cornell University, New York, New York 10021

Abstract. Ezrin, a member of the ezrin/radixin/moesin (ERM) family, localizes to microvilli of epithelia in vivo, where it bridges actin filaments and plasma membrane proteins. Here, we demonstrate two specific morphogenetic roles of ezrin in the retinal pigment epithelium (RPE), i.e., the formation of very long apical microvilli and of elaborate basal infoldings typical of these cells, and characterize the role of ezrin in these processes using antisense and transfection approaches. In the adult rat RPE, only ezrin (no moesin or radixin) was detected at high levels by immunofluorescence and immunoelectron microscopy at microvilli and basal infoldings. At the time when these morphological differentiations develop, in the first two weeks after birth, ezrin levels increased fourfold to adult levels. Addition of ezrin antisense oligonucleotides to primary cultures of rat RPE drastically decreased both apical microvilli and basal infoldings. Transfection of ezrin cDNA into the RPE-J cell line, which has only trace amounts of ezrin and moesin, sparse and stubby apical microvilli, and no basal infoldings, induced maturation of microvilli and the formation of basal infoldings without changing moesin expression levels. Taken together, the results indicate that ezrin is a major determinant in the maturation of surface differentiations of RPE independently of other ERM family members.

Key words: antisense • retinal development • cortical cytoskeleton • epithelia • ezrin radixin moesin proteins

THE cortical actin cytoskeleton is a highly dynamic structure that participates in the morphogenesis of a variety of surface differentiations under the control of defined signal transduction pathways. The ezrin/radixin/moesin (ERM)[1] family consists of ezrin (Bretscher, 1983), radixin (Tsukita et al., 1989a,b; Funayama et al., 1991), and moesin (Lankes and Furthmayr, 1991). These proteins, as well as band 4.1, talin, and the neurofibromatosis tumor suppressor merlin or schwannomin, among other proteins, share an NH_2-terminal domain, denominated FERM domain (Chishti et al., 1998; Girault et al., 1998; Mangeat et al., 1999). The closely related ERM proteins (>75% amino acid sequence identity) localize just beneath the plasma membrane to areas where actin filaments are densely concentrated, i.e., microvilli, ruffling membranes, cleavage furrows, and cell–cell and cell–substrate adhesion sites. The results of many studies support a model in which ERM proteins function as highly regulated cross-linkers between plasma membrane proteins and the cortical actin cytoskeleton. The NH_2-terminal domain of ERM proteins is highly homologous within the group (>85% identity) and has been reported to interact with the hyaluronate receptor CD44 (Tsukita et al., 1994); a novel family of 50-kD ERM binding proteins containing PDZ domains, which includes EBP50 (Reczek et al., 1997); the regulatory subunit RII of protein kinase A (Dransfield et al., 1997); the Rho-GDP dissociation inhibitor, Rho-GDI (Hirao et al., 1996); and other proteins (see Bretscher, 1999 and Mangeat et al., 1999 for recent reviews). On the other hand, their COOH terminus, particularly the terminal 34 amino acids, binds the actin cytoskeleton (Algrain et al., 1993; Arpin et al., 1994; Turunen et al., 1994; Pestonjamasp et al., 1995; Yao et al., 1996).

The ERM proteins undergo phosphorylation and are involved in morphogenetic changes and reorganization of the cytoskeleton in response to stimuli mediated by serine/threonine and tyrosine kinases (Bretscher, 1989, 1999; Mangeat et al., 1999). In the unphosphorylated state, the ERM proteins are present as monomers and have no exposed sites for interaction with other proteins or the actin cytoskeleton, due to intramolecular and/or intermolecular

Address correspondence to Enrique Rodriguez-Boulan, Dyson Vision Inst., Dept. of Ophthalmology, Weill Medical College of Cornell University, 1300 York Avenue, New York, NY 10021. Tel.: (212) 746-2272. Fax: (212) 746-8101. E-mail: boulan@mail.med.cornell.edu

1. *Abbreviations used in this paper:* ERM, ezrin/radixin/moesin family; HGF, hepatocyte growth factor; P, postnatal day; PR, photoreceptor; pAb, polyclonal antibody; RPE, retinal pigment epithelium; VSVG, vesicular stomatitis virus glycoprotein G.

interactions between the NH_2- and the COOH-terminal domains. Phosphorylation of a COOH-terminal threonine residue present in all ERM proteins by Rho-kinase (Takahashi et al., 1997; Matsui et al., 1998; Shaw et al., 1998) or protein kinase C theta (Pietromonaco et al., 1998; Simons et al., 1998) frees the COOH- and NH_2-terminal domains without affecting F-actin binding. On the other hand, within minutes phosphorylation by tyrosine kinases leads to the generation of oligomers, either homotypic or heterotypic (with other ERM proteins) and tight association with the cytoskeleton (Bretscher, 1999; Mangeat et al., 1999). Phosphorylation of ezrin correlates with dramatic changes in cell morphology and behavior, such as the generation of microvilli from intracellular canaliculi and tubules upon stimulation of HCl secretion by parietal cells (Hanzel et al., 1991) and hepatocyte growth factor (HGF)/scatter factor-induced cell migration and tubulogenesis (Crepaldi et al., 1997). Conversely, overexpression of the NH_2-terminal domain of the ezrin molecule in the kidney LLC-PK cell line decreased the number of microvilli and made the cells unresponsive to HGF (Crepaldi et al., 1997). Furthermore, incubation of mouse epithelial and thymoma cells or primary neuronal culture in the presence of a mixture of antisense oligonucleotides complementary to ERM proteins promoted loss of cell–cell and cell–substrate adhesion, as well as the disappearance of microvilli (Takeuchi et al., 1994) or inhibition of growth cone extension (Paglini et al., 1998).

While the studies mentioned suggest important roles of ERM proteins in the formation of actin based structures at the plasma membrane, they fall short of elucidating the specific functions of individual ERM proteins. As the NH_2-terminal region is highly homologous in all ERM proteins, it can interact with the COOH terminus of other family members. Since most cultured cell lines show promiscuous expression of two to three members of the ERM group, the NH_2-terminal ezrin peptide, studied by Crepaldi et al. (1997), likely affected, and may have inhibited, moesin and/or radixin in addition to ezrin. In the experiments by Takeuchi et al. (1994) and Paglini et al. (1998), the morphogenetic effects of ERM antisense oligonucleotides in cells were only observed when they were applied in combination. Addition of individual antisense oligonucleotides to ezrin or radixin caused only marginal inhibition of cell–cell and cell–substrate adhesion, whereas antisense oligonucleotides to moesin only mildly affected microvilli structures. Perhaps the most specific approach to disrupt ezrin function was its functional ablation by micro-CALI (chromatophore-assisted laser irradiation) in transformed fibroblasts, which led to the collapse of pseudopodia structures of these cells and pointed to a critical role of ezrin in fibroblast cell shape and motility (Lamb et al., 1997). However, in vivo ezrin expression is mainly observed in epithelial cells. In contrast with their promiscuous expression in cultured cell lines, the tissue distribution of ERM proteins in vivo appears to be tightly regulated and complementary. Ezrin is detected at the apical microvilli of various epithelia, moesin is expressed mostly by endothelial cells (Berryman et al., 1993; Schwartz-Albiez et al., 1995) and radixin is enriched in hepatic adherent junctions and in cardiac intercalated discs (Tsukita et al., 1989a).

The retinal pigment epithelium (RPE) performs highly specialized metabolic and transport functions essential for homeostasis of the neural retina (Bok, 1993). The apical surface of RPE cells emits very long and thin microvilli that interdigitate with the adjacent photoreceptor (PR) outer segments, providing mechanical support and carrying out the diurnal phagocytic removal of spent PR tips (one RPE cell supports 30–50 PR, which shed daily ~5% of their outer segment mass). The basal surface of RPE cells displays highly convoluted basal folds that attach to a specialized Bruch's basement membrane and participate in extensive metabolic exchanges with the blood vessels in the underlying choriocapillaris (Zinn and Benjamin-Henkind, 1979). RPE cells and PR undergo dramatic postnatal maturation in the rat. At birth, PR outer segments are missing and the RPE is immature, with very short apical microvilli and a smooth basal membrane. Within two weeks, outer segments mature and the RPE forms its characteristic long microvilli and convoluted basal infoldings (Braekevelt and Hollenberg, 1970; Marmorstein et al., 1998).

The morphological variations observed in microvillar shape in different tissues reflect the different complement of actin-associated proteins (such as myosin, tropomyosin, fimbrin, villin, and α-actinin, among others). RPE microvilli possess an internal core bundle of densely packed actin filaments (Drenckhahn and Wagner, 1985; Vaughan and Fisher, 1987). Previous studies detected myosin VIIa at the base of apical processes (Hasson and Mooseker, 1995; Liu et al., 1997), but failed to detect villin, fimbrin, and myosin I (Hofer and Drenckhahn, 1993). Another study showed that RPE actin bundles were not affected by Ca^{2+} concentration, suggesting that other villin-like proteins may not be present (Owaribe and Eguchi, 1985). Because RPE microvilli express high levels of ezrin (Hofer and Drenckhahn, 1993), we hypothesized that this protein might play a role in the postnatal maturation of RPE microvilli. We studied the developmental expression of ERM proteins during RPE maturation and carried out antisense experiments in primary RPE cultures that preserve long microvilli and basal infoldings (Stramm et al., 1983; Heth et al., 1987; Gundersen et al., 1993; Davis et al., 1995). In addition, we overexpressed ezrin in the rat RPE cell line RPE-J, which has few and short microvilli and no basal infoldings (Nabi et al., 1993; Bonilha et al., 1997; Marmorstein et al., 1998). Our results are consistent with a key role of ezrin in RPE morphogenesis. Although moesin expression was stimulated under culture conditions, the results suggest only a limited role in RPE cells in vitro, consistent with its absence from RPE in vivo.

Materials and Methods

Reagents and Antibodies

Reagents were from Sigma Chemical Co. or GIBCO BRL, unless otherwise stated. mAb3056 to the COOH-terminal domain of ezrin was purchased from Chemicon. Polyclonal ezrin antibody was a generous gift from Dr. Monique Arpin (Curie Institute, Paris, France). Antiezrin polyclonal antibody (pAb) C-19 directed to the peptide 566–584 of human ezrin (conserved in all ERM proteins) was purchased from Santa Cruz Biotechnology, Inc. Affinity-purified polyclonal moesin antibody was a generous gift from Dr. Anthony Bretscher (Cornell University, Ithaca,

NY). Polyclonal antibodies to radixin (457 and 220) were generously provided by Dr. Frank Solomon (MIT, Cambridge, MA). mAb to vesicular stomatitis virus glycoprotein G (VSVG), clone P5D4, raised against the 11-amino acid COOH terminus of the VSVG was previously described (Kreis, 1986). Secondary antibodies were purchased from Cappel Laboratories or Jackson ImmunoResearch Laboratories, Inc.

Cell Culture

RPE-J cells were originally obtained from rat RPE by immortalization with temperature sensitive SV40 T antigen (Nabi et al., 1993). The cells were cultured at the permissive temperature of 32°C in DME medium supplemented with 4% heat-inactivated CELLect Gold FCS (ICN Pharmaceuticals, Inc.), L-glutamine, nonessential amino acids, and antibiotics. To promote differentiation, cells were plated on polycarbonate Transwell filters (Costar) coated with a thin layer of Matrigel (Collaborative Research). The cells were then cultured in growth medium supplemented with 10^{-8} M retinoic acid for 6 d, and then switched to 40°C, the nonpermissive temperature for transformation, for 36–48 h (Nabi et al., 1993).

Primary RPE cultures were prepared from 2-wk-old Long Evans rats (Harlan Sprague Dawley). Animals were killed by CO_2 asphyxiation, the eyes were enucleated and stored in HBSS. A circumferential incision was made above the ora serrata, and the cornea, lens, iris, and vitreous body were removed. The eyecups with the neural retina exposed were incubated in 320 U/ml hyaluronidase in HBSS for 1 h at 37°C, the neural retina was peeled off from the RPE, and the eyecups were incubated in 2 mg/ml trypsin in HBSS for 60 min at 37°C. RPE sheets were teased from the underlying choroid with needles, collected, and incubated with trypsin/EDTA for 1 min. The cells were plated on Matrigel-coated Transwell filters and cultured without further passaging in DME supplemented with 10% FCS, L-glutamine, nonessential amino acids, and antibiotics.

Phosphorothioate Antisense Oligonucleotide Treatment

Phosphorothioate antisense oligonucleotides used in this study were complementary to the position −4 to 20 (relative to the translation initiation site) of rat ezrin mRNA (GenBank/EMBL/DDBJ, X67788; Barila et al., 1995). Oligonucleotides were purchased from Cornell University and Operon Technologies, Inc. Sense oligonucleotides corresponding to positions −4 to 20 were used as controls. The antisense oligonucleotide sequence was analyzed with the BLAST sequence database and did not show significant homology with other known sequences. Primary RPE cells on 6.5-mm diam Transwell filters were treated with oligonucleotide as described by Takeuchi et al. (1994). In brief, 20 μM oligonucleotides were added into the culture medium of the apical chamber every 4 h for 96 h. Every four additions, the culture medium was exchanged with fresh medium containing 20 μM oligonucleotide. The antisense effects described were neutralized by the addition of the same concentration of sense oligonucleotide.

Ezrin Transfection

VSVG-tagged cDNA coding for the wild-type human ezrin, a generous gift of Dr. Monique Arpin (Curie Institute, Paris, France), was previously described (Algrain et al., 1993). RPE-J cells were seeded on 10-cm petri dishes 24 h before transfection using a standard calcium precipitate protocol (Chen and Okayama, 1988). Transfected cells were selected in medium containing 0.6 mg/ml G-418. Three clones, which produced the exogenous ezrin at different levels (as determined by immunoblots) were selected for further studies.

Cryosections

CO_2 anesthetized Long Evans rats of different ages had an intracardiac perfusion with 4% paraformaldehyde made in PBS supplemented with 0.3 mM $CaCl_2$ and 1 mM $MgCl_2$ (PBS/CM). Their eyes were enucleated and postfixed by immersion in the same fixative overnight. Eyecups were infused successively with 10 and 20% sucrose in PBS/CM, and with Tissue-Tek "4583" (Miles Inc.). 10-μm cryosections were cut on a cryostat (Bright Instrument Company) and collected on SuperFrost slides (Fisher).

Immunofluorescence Microscopy

Cells on filters were fixed in 4% paraformaldehyde in PBS/CM for 20 min, quenched in 50 mM NH_4Cl in PBS/CM for 20 min, and permeabilized in 0.2% Triton X-100 in PBS/CM for 10 min. After blocking in PBS/CM supplemented with 0.2% BSA (PBS/CM/BSA) for 30 min, the filters and cryosections were incubated with the ezrin monoclonal or polyclonal antibodies, moesin pAb, or VSVG mAb in PBS/CM/BSA for 1 h. The samples were washed in PBS/CM/BSA and incubated with secondary antibodies coupled to FITC or Cy™3 for 45 min. Cell nuclei were labeled with 1 μg/ml 4′,6-diamidino-2-phenylindole in PBS/CM for 5 min, or with 2 μg/ml propidium iodide in PBS/CM for 15 min. 1-μm X-Y (en face) or X-Z (transverse) sections were obtained using a dual channel laser scanning confocal microscope (Sarastro, Molecular Dynamics). Alternatively, samples were analyzed using an epifluorescence microscope (model E600; Nikon). Digital images were collected with a cooled CCD camera and Metamorph software (Universal Imaging). Microscopic panels were composed using Adobe Photoshop 5.0.

Electron Microscopy

Freshly isolated rat eyecups of different ages, primary RPE, RPE-J, and RPE-J clones plated on filters were fixed in 2.5% glutaraldehyde, 0.2% picric acid in 0.1 M cacodylate buffer, pH 7.3. Samples were postfixed in 1% osmium tetroxide for 1 h, dehydrated in acetone and embedded in Epon. Ultrathin sections were stained with uranyl acetate and lead citrate. Specimens were examined at 80 kV in a JEOL 100 CXII electron microscope. For scanning EM, samples were plated on 1% Alcian blue-treated (Sigma Chemical Co.) glass coverslips, fixed in 2.5% glutaraldehyde freshly diluted in 0.1 M cacodylate buffer, postfixed in 1% osmium tetroxide for 30 min, dehydrated in graded ethanol solutions, critical point-dried in liquid carbon dioxide, coated with vacuum-evaporated gold-platinum, and examined in a JEOL 100 CXII microscope equipped with the ASID high resolution scanning module, using an accelerating voltage of 20 kV.

Immunoelectron Microscopy

Freshly isolated rat eyecups of adult rats were fixed in 4% paraformaldehyde, 0.1% glutaraldehyde, 0.2% picric acid in 0.1 M modified PHEM buffer, pH 6.9 (60 mM Pipes, 20 mM Hepes, 10 mM EGTA, 5 mM $MgCl_2$, 70 mM KCl), for 1 h at 4°C. Samples were postfixed in 0.25% tannic acid for 1 h at 4°C, dehydrated in ethanol, embedded in Unicryl Kit resin (Ted Pella Inc.), and polymerized under UV light for 96 h at −20°C. Ultrathin sections on grids were hydrated at room temperature for 1 h with PBS, 1% BSA, 0.01% Tween 20, 10% goat serum, and incubated in 50 mM NH_4Cl in PBS/CM for 30 min, followed by sequential incubation with antiezrin rabbit antibody (1:100) and 10-nm colloidal gold-conjugated antibody (Ted Pella Inc.) for 1 h each.

Quantification of Ezrin in Cell Lysates

Whole cell lysates from RPE-J monolayers, RPE collected from rat eyecups, and primary cultures of RPE were solubilized in PBS supplemented with 2% SDS and a cocktail of protease (1 mM PMSF, 20 μg/ml leupeptin, 20 μg/ml pepstatin A, and 40 μg/ml aprotinin) and phosphatase (100 μM sodium vanadate) inhibitors. 10 μg of total protein of each sample was resolved in a 7.5% SDS-PAGE and electrotransferred to nitrocellulose membranes (Schleicher & Schuell). To detect ezrin and moesin, membranes were incubated with polyclonal ezrin antibody C-19 in Blotto A buffer (20 mM Tris/HCl, 0.9% NaCl, 0.05% Tween 20, 5% skimmed milk) as directed by the manufacturer. Protein detection was performed with secondary antibodies conjugated to peroxidase and visualized using the Western blot chemiluminescence Reagent Plus (New England Nuclear Life Science Products, Inc.) detection system. The intensity of scanned protein bands was analyzed with NIH Image 1.62 software.

Detergent Extraction of Ezrin

Association of ezrin with the cytoskeleton was defined by immunofluorescence and cell fractionation into detergent soluble and insoluble fractions as previously described (Crepaldi et al., 1997; Kreis, 1987). For immunofluorescence, plated cells were washed in PBS/CM and dipped four times for 5 s at room temperature in four different beakers containing extraction buffer MES (50 mM MES, 3 mM EGTA, 5 mM $MgCl_2$, 0.5% Triton X-100, pH 6.4), fixed in 4% paraformaldehyde, and processed for immunofluorescence as described above. Alternatively, cells seeded on 6.5-mm Transwell filters were extracted in 300 μl extraction buffer MES for 40 s at room temperature. Detergent-soluble fractions were precipitated in 80% acetone for at least 4 h at −20°C, and centrifuged at 300 *g* for 10 min at 4°C. Detergent soluble and insoluble fractions were resuspended in 30 μl

of Laemmli sample buffer each, loaded, and analyzed by 7.5% SDS-PAGE and immunoblotting.

Results

Expression of Ezrin during Postnatal Development of RPE Microvilli

RPE cells and the neighboring PR undergo dramatic shape changes during postnatal maturation of the retina in the rat. Histological and fluorescence analysis of the immature rat eyecup at postnatal day 2 (P2; Fig. 1, A–C) shows RPE cells in direct contact with the immature PR, identified by their nuclei (stained blue in Fig. 1 A, and red [with propidium iodide] in Fig. 1, B and C), as the outer segments of the PR have not developed yet (see Fig. 1, A–C). In contrast, in animals two weeks of age or older, the mature retinal architecture and interactions have been established (Fig. 1, D–F) and the RPE is separated from the outer nuclear layer and the inner PR segments by well developed PR outer segments. Immunofluorescence of rat eyecup cryosections detected ezrin at the apical surface of both immature (Fig. 1 B) and adult (Fig. 1 E) RPE cells. Upon RPE maturation, apical ezrin staining was more intense; in the adult retina, it was observed in the external regions of the PR layer (Fig. 1 E), where RPE microvilli ensheath the fully developed outer segments. Parallel cryosections of P2 (Fig. 1 C) and adult (Fig. 1 F) retina stained with a specific moesin antibody failed to detect it at the RPE layer. Some moesin staining was detected in the capillaries at the choroid layer underneath the RPE layer at both stages of development. Moreover, the labeling of the same cryosection with pAb 457 specific to mouse radixin failed to detect it at the RPE layer (data not shown).

The structural changes associated with RPE maturation, visible by EM, are shown in Fig. 2. The RPE of the newborn rat displays short and stubby apical microvilli and very short invaginations and tubules in association with its basal plasma membrane (Fig. 2 A). By P7, halfway through maturation, the apical surface has extended long microvilli whereas the basal surface has developed immature basal infoldings (Fig. 2 B). By P14, rat RPE displays apical microvilli and maximally developed basal infoldings (data not shown), identical to those found in the RPE of the adult rat (Fig. 2 C). Previous morphometric studies of rat eyecups of different ages have shown that both apical and basolateral surfaces of RPE double their area during postnatal maturation (Marmorstein et al., 1998).

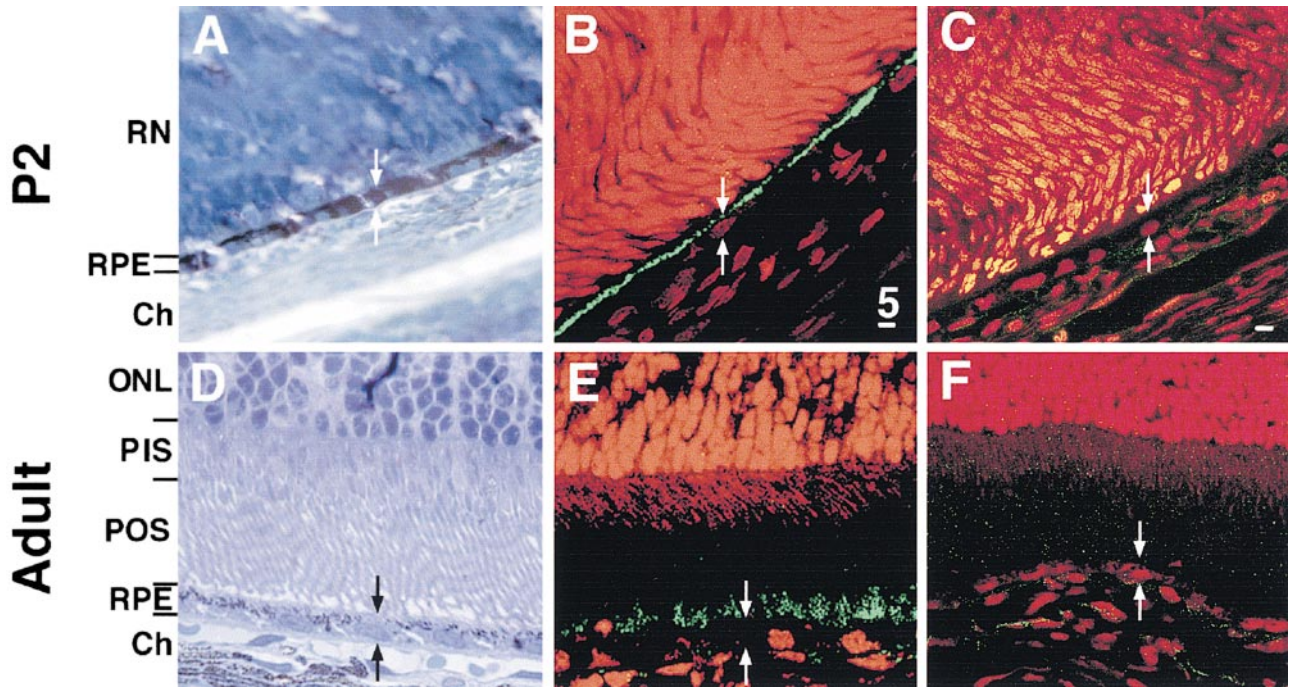

Figure 1. Ezrin localizes to the apical surface of rat RPE during postnatal maturation. RPE cells undergo a dramatic change in their morphology during postnatal maturation of the retina, which also includes the formation of PR outer segments. Observation of thick sections of epon-embedded immature (P2, A) and mature (Adult, D) eyes stained with Toluidine blue highlights the cell layers present in each situation. Immature RPE cells are very close apically to the immature retinal nuclei (RN) and interact basally with the choroid (Ch). On the other hand, fully differentiated RPE cells interact apically with the PR outer segments (POS). For ezrin immunolocalization, tissues were fixed by intracardiac perfusion with 4% paraformaldehyde. 10-μm cryosections of eyecups were labeled with a mAb to ezrin (B and E), while parallel sections were stained with a pAb directed to moesin (C and F). Cell nuclei were labeled with propidium iodide. The labeled cryosections were analyzed by dual channel laser scanning confocal microscopy. Immature (B) and mature (E) RPE cells displayed ezrin localization almost exclusively at the apical RPE surface. Neither immature (C) nor mature (F) RPE cells display any moesin staining. Moesin staining was detected in the underlying choroid. Ch, choroid; ONL, outer nuclear layer; PIS, PR inner segments; POS, PR outer segments; RN, immature retinal nuclei. Bar, 5 μm.

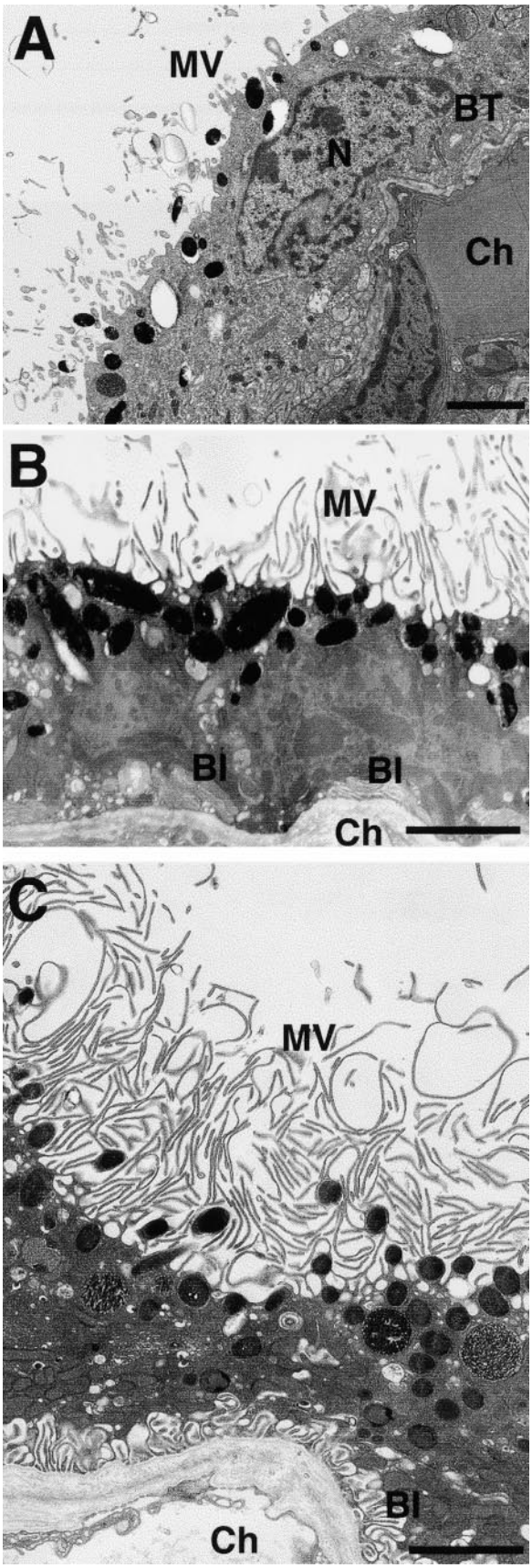

Figure 2. Ultrastructural maturation of the retinal pigment epithelium. Neural retina-free eyecups were fixed in 2.5% glutaraldehyde + 0.2% picric acid made in 0.1 M cacodylate buffer, and processed for transmission EM. A, The newborn RPE (P2) has very short microvilli extending from its apical surface. Its basal surface interacts with the choriocapillaris through the relatively smooth Bruch's basement membrane. Cytoplasmic tubular structures (BT) can be observed connected to the basal surface. B, At P7, longer microvilli emerge from the apical surface. The basal surface displays deep basal infoldings in some areas. C, In the mature rat eye, RPE cells extend remarkably thin and long microvilli from their apical surfaces. BI, basal infoldings; BT, basal tubules; Ch, choroid; MV, microvilli; N, nucleus. Bars, 2 μm.

Immunoelectron Microscopy Localizes Ezrin to Apical Microvilli and Basal Infoldings of Mature RPE In Vivo

Postembedding immunocytochemistry of adult eyecups was used to further examine the ultrastructural localization of ezrin in RPE cells. Ultrathin sections of adult eyecups embedded in unicryl were sequentially labeled with an affinity-purified pAb to ezrin, followed by a secondary donkey anti–rabbit IgG antibody conjugated with colloidal-gold particles. In these samples, labeling was specifically associated with actin bundles in apical microvilli (Fig. 3 A, arrowheads) and, to a lower extent, with basal infoldings (Fig. 3 B). Importantly, no ezrin labeling was associated with the apical plasma membrane adjacent to the microvilli. A similar ezrin distribution was observed in primary cultures of mature RPE cells plated on semipermeable polycarbonate filters (data not shown). Control samples labeled with secondary antibody alone showed no labeling (data not shown). These data demonstrate that ezrin has a dual apical and basal distribution in RPE cells in vivo, as in parietal cells of gastric glands (Hanzel et al., 1991), but, unlike most other epithelia, where it is usually only found at apical microvilli (Berryman et al., 1993).

Ezrin Expression Levels Increase as RPE Develop Apical Microvilli and Basal Infoldings

If ezrin is involved in the process of RPE maturation, it may be upregulated during this time. Immunoblots of lysates of RPE cells obtained from rats of different postnatal ages demonstrated a progressive increase in ezrin with adult levels observed after two weeks (Fig. 4 A). Quantitation of these blots showed that ezrin expression was upregulated ~400% between P2 and adults (Fig. 4 B). In contrast, moesin and radixin, also reactive with the pAb used in these studies, were not detected in either developing or adult RPE. These data are in agreement with our immunofluorescence data which detected neither moesin (Fig. 1) nor radixin (data not shown) in RPE in vivo. The large increase of ezrin expression during postnatal maturation of RPE further suggested that this protein may indeed play an important role in the establishment of apical and basal actin-based structures.

Primary RPE Cultures Express Ezrin Mostly Bound to their Apical Cytoskeleton Whereas Moesin Is Mostly Bound to their Basolateral Cytoskeleton

Primary RPE cultures preserve long microvilli and basal infoldings characteristic of adult RPE in the adult eye (Stramm et al., 1983; Heth et al., 1987; Gundersen et al., 1993; Davis et al., 1995). Even when RPE in situ expressed

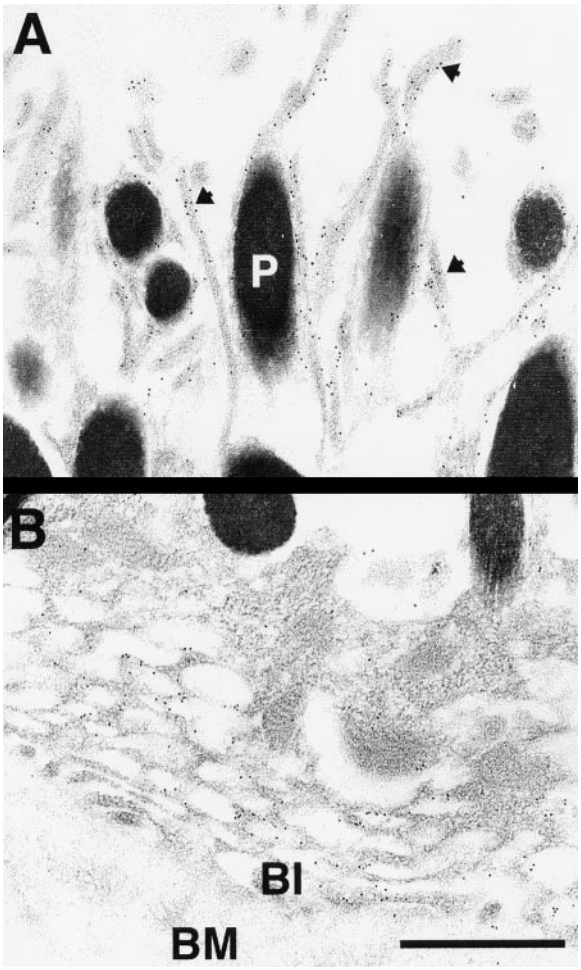

Figure 3. Ezrin localizes both at RPE apical microvilli and basal infoldings. Adult neural retina-free eyecups were fixed in a mix of 4% paraformaldehyde, 0.1% glutaraldehyde, and 0.2% picric acid prepared in PHEM modified buffer. Tissue was sequentially dehydrated in ethanol, embedded in Unicryl, and polymerized at −20°C under UV light. Ultrathin sections were sequentially reacted with a polyclonal antiezrin antibody and a gold-conjugated (10 nm) donkey anti–rabbit antibody. In these samples, labeling was specifically associated with apical microvilli (A) and to a lower extent with basal infoldings (B). Arrowheads point to colloidal gold/ezrin antibodies decorating microvilli. BI, basal infoldings; BM, Bruch's membrane; P, pigment granule. Bar, 0.5 μm.

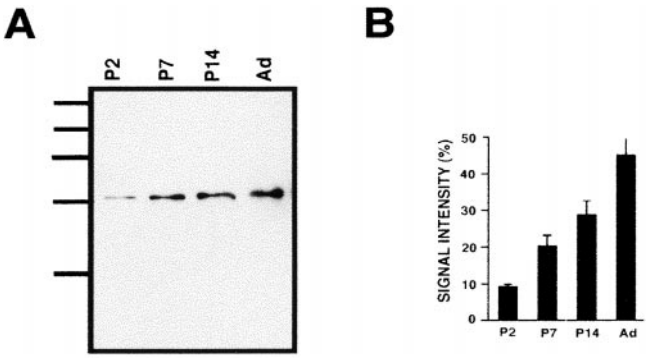

Figure 4. Ezrin expression increases during postnatal maturation of RPE. A, RPE of different ages (P2 to adult [Ad]) were harvested and lysed in 2% SDS in PBS supplemented with protease inhibitors and 100 μM sodium orthovanadate. 10 μg of protein of each sample was separated in a 7.5% SDS gel, transferred to nitrocellulose membranes and probed with a pAb specific to a COOH-terminal peptide common to all ERM proteins, followed by ECF detection of immunoreactivity. B, Membranes were exposed to film and ezrin signal intensities were analyzed with NIH Image 1.62 software and plotted. During RPE maturation, ezrin expression is upregulated fourfold. Data shown are the mean of four independent experiments ± SEM. The large error bar associated with the adult samples is due to apical surface damage during the enzymatic peeling of the neural retina from the RPE.

only ezrin, we tested the primary RPE cultures for the expression of other ERM proteins, as it is well known that their expression is more promiscuous under culture conditions. Primary RPE monolayers were probed with an antibody specific to a COOH-terminal peptide conserved in all three ERM proteins. Whole extracts of these cells revealed the presence of two bands corresponding to the molecular weight of ezrin and moesin (Fig. 5 A, lane 1, arrows); no band with the molecular weight of radixin (intermediate between ezrin and radixin) was detected. Quantification of ezrin and moesin from the Western blot indicated a 1.7:1 ratio between these two proteins. To test the association of ezrin and moesin with the cytoskeleton, we carried out detergent extractions. 45 ± 1.0% of ezrin and 52 ± 3.5% of moesin in primary RPE were extracted (Fig. 5 A, lanes 2 [soluble] and 3 [insoluble]), indicating that a large fraction of each protein was apparently linked to the cytoskeleton.

We analyzed the distribution and detergent extractability of ezrin and moesin in primary RPE monolayers by immunofluorescence (Fig. 5, B–I). Confocal microscopy en face examination of paraformaldehyde-fixed monolayers grown on polycarbonate filters revealed an apical punctate staining for ezrin consistent with an apical localization, similar to that observed in RPE in situ (Fig. 5 B). Cross-sections of these monolayers confirmed the apical localization of ezrin (Fig. 5 C). Confocal immunofluorescence analysis of primary RPE cultures first extracted with 0.5% Triton X-100 and then fixed with paraformaldehyde, revealed the presence of ezrin, primarily in apical regions consistent with the association with apical microvilli (Fig. 5, D and E). On the other hand, moesin appeared to be associated with apical, lateral, and basal surfaces of primary RPE cells fixed before extraction (Fig. 5, F and G), but only on the basal surface of cells extracted with 0.5% Triton X-100 before fixation with paraformaldehyde (Fig. 5, H and I). Incubation of primary RPE monolayers with an antibody specific to radixin failed to stain the cells (data not shown). The data suggest that in primary RPE cultures, a major pool of ezrin is associated with the apical surface of the cells, while the most stable pool of moesin interacts with basolateral membranes.

Treatment of Primary RPE with Ezrin Antisense Oligonucleotides Abolishes Apical Microvilli and Basal Infoldings

To test the hypothesis that ezrin is an important player in

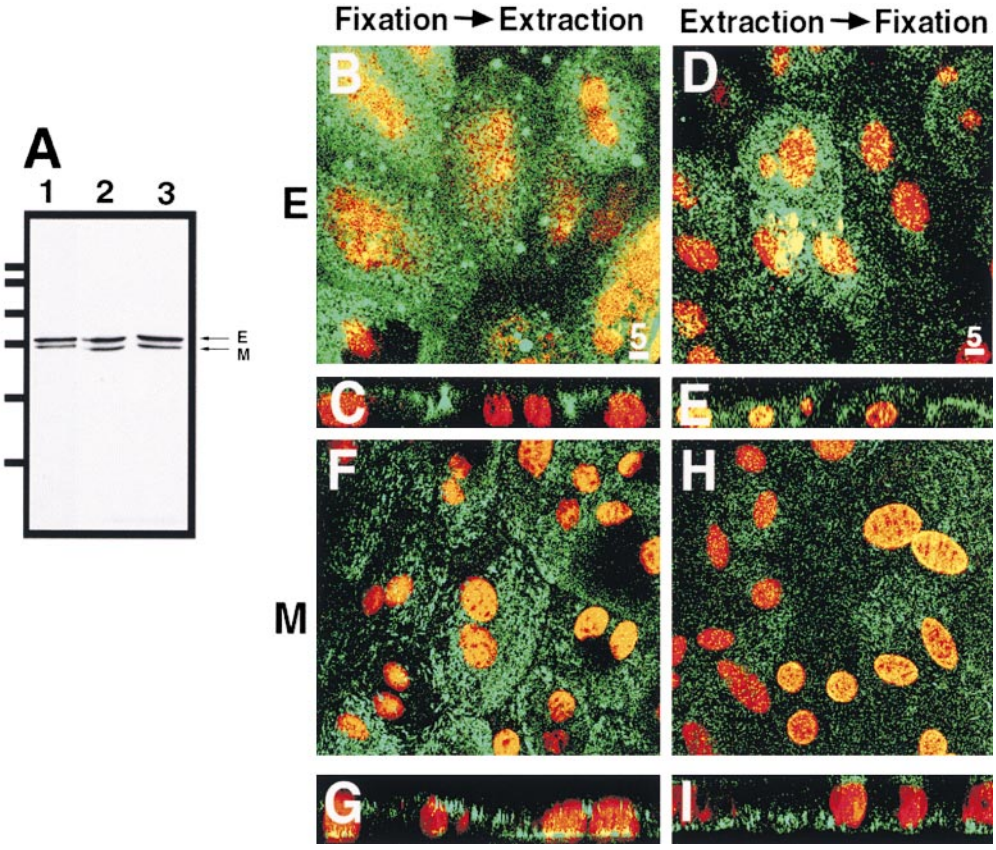

Figure 5. Ezrin localizes mostly to the apical surface of primary RPE cells whereas moesin localizes mostly to the basal surface. Primary RPE monolayers were probed with an antibody specific to a COOH-terminal peptide conserved in all three ERM proteins. Whole extracts (10 μg) of these cells revealed the presence of two bands corresponding to the molecular weight of ezrin and moesin (A, lane 1, arrows), but no band corresponding to radixin, with intermediate mobility between the two other proteins. Analysis of Triton-extracted fractions from primary RPE cultures (20–30 μg and ~60–80 μg protein per lane in the detergent soluble and insoluble fractions, respectively) showed that 45 ± 0.5% of ezrin and 52 ± 3.5% of moesin were extracted (A, lanes 2 [soluble] and 3 [insoluble]). Values reported are the mean of three independent experiments ± SEM. Differentiated monolayers plated on filters were fixed with paraformaldehyde, permeabilized with Triton X-100 for 10 min, and labeled either with an mAb to ezrin (E; B–E) or a pAb to moesin (M; F–I). Nuclei were stained with propidium iodide. Samples were observed using a dual channel laser scanning confocal microscope. B, Paraformaldehyde-fixed monolayers grown on polycarbonate filters displayed a punctate ezrin staining suggestive of an apical localization in primary RPE cultures. C, The apical localization of ezrin was confirmed in Z-scans performed through the monolayer. D and E, Confocal immunofluorescence analysis of primary RPE cultures extracted with 0.5% Triton X-100 and fixed with paraformaldehyde, revealed the presence of ezrin, primarily in apical microvilli, indicating that ezrin resisted nonionic detergent extraction mostly at the apical surface of the cells. F, On the other hand, moesin was more evenly distributed in the primary cells. G, Vertical section of the monolayers confirmed moesin distribution in the apical, lateral, and basal surface of primary RPE cells. H, Observation of cells extracted with 0.5% Triton and then fixed with paraformaldehyde, revealed that there was a decrease of moesin staining corresponding to moesin detergent extraction. I, Cross-sections through the monolayers revealed that the majority of moesin resistant to detergent extraction is localized to the basal surface of the cells suggesting that in these cells, moesin is weakly or not anchored to the apical cytoskeleton. Bar, 5 μm.

the establishment of apical microvilli and basal infoldings, we used an antisense oligonucleotide approach. Primary RPE cultures were exposed for 96 h to antisense oligonucleotides directed to the first 24 amino acids encoded by the rat ezrin mRNA (Fig. 6). In control RPE cultures not exposed to antisense oligonucleotides, the expression level of ezrin, measured by immunoblot, was high, similar to that of RPE cells obtained directly from the retina for analysis (Fig. 6 A, lane 1). As previously shown, moesin was also expressed. Importantly, addition of sense oligonucleotides did not affect either ezrin or moesin expression in these cells (Fig. 6 A, lane 2). In contrast, primary RPE monolayers cultured in the presence of ezrin antisense oligonucleotides displayed an almost complete inhibition of ezrin expression relative to untreated control cells, whereas moesin expression was not affected or was inhibited to a much smaller extent (Fig. 6 A, lane 3). In control experiments, addition of sense plus antisense oligonucleotides directed to ezrin resulted in levels of expression of both ezrin and moesin similar to control levels (data not shown). The effects of ezrin antisense oligonucleotides were also examined by immunofluorescence (Fig. 6, B–G). Control primary RPE cells displayed a typical microvillar apical staining pattern for ezrin, consisting of punctate or short linear elements frequently coalescing into clumps (Fig. 6 B). Instead, moesin expression was diffuse throughout the cytoplasm with small puncta of undefined origin not associated with the apical surface (Fig. 6 C). No change in the ezrin (Fig. 6 D) or moesin (Fig. 6 E) labeling patterns was observed when monolayers were supplemented with ezrin sense oligonucleotides or with a mixture of sense and antisense oligonucleotides (data not shown). In sharp contrast, monolayers supplemented with ezrin antisense oligonucleotides almost completely lost the ezrin staining (Fig. 6 F), whereas moesin staining remained largely unchanged (Fig. 6 G).

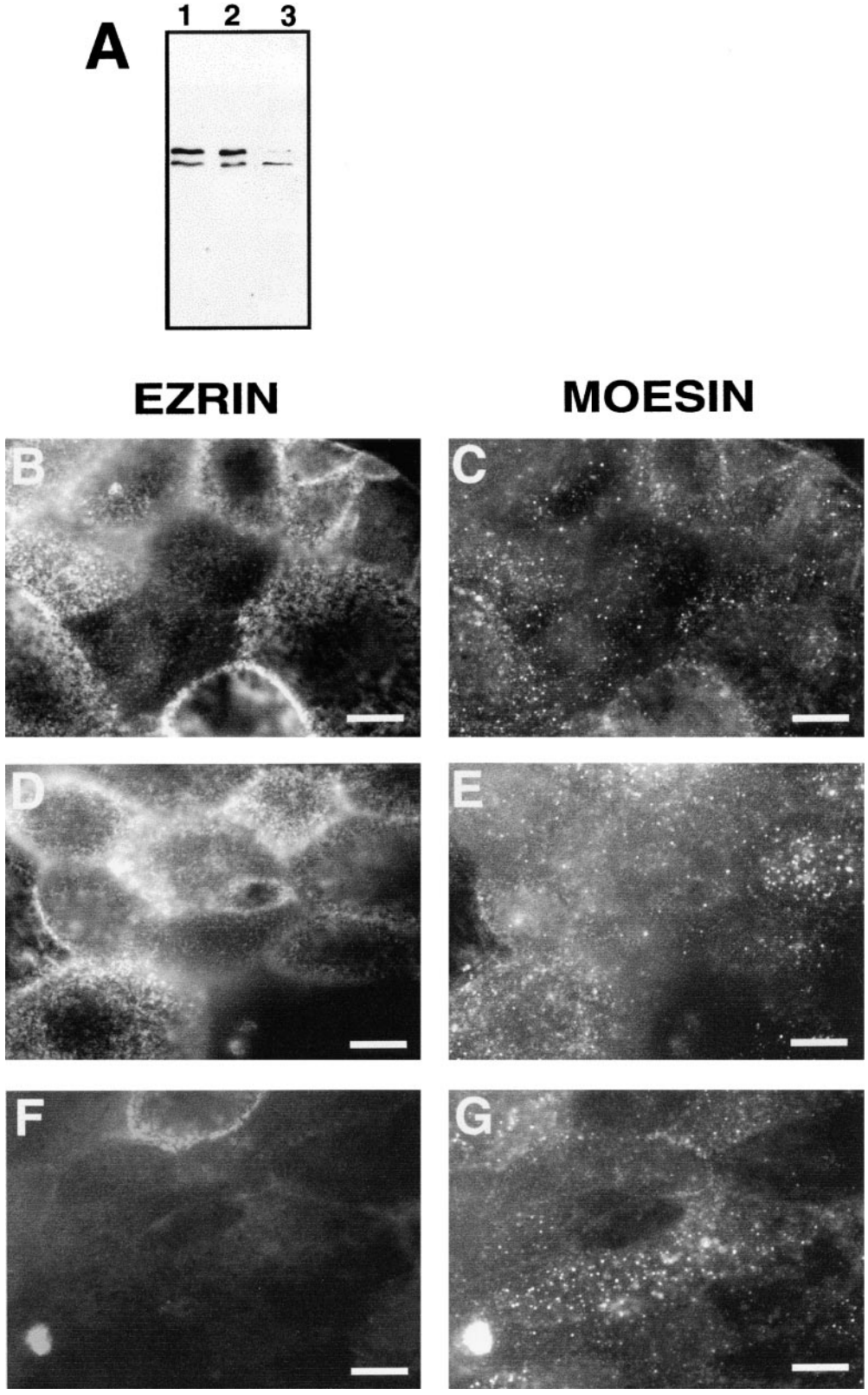

Figure 6. Treatment of primary RPE monolayers with ezrin oligonucleotides decreases ezrin expression and disrupts RPE microvilli. Immunoblot and immunofluorescence. Primary cultures of rat RPE were plated on filters. Cultures were supplemented with 20 μM sense or antisense oligonucleotides directed to ezrin for 96 h. At the end of this period, filters were cut in two pieces and processed separately. A, Half of filters were lysed in 2% PBS plus protease and phosphatase inhibitors and were biochemically analyzed. Antisense treated monolayers (lane 3) showed a 80% decrease in ezrin levels when compared with control (lane 1) and sense (lane 2) treated monolayers. The other half of the samples were permeabilized with 0.02% Triton X-100 for 10 min, fixed with paraformaldehyde, and processed for double immunofluorescence for ezrin and moesin. Samples were observed using an epifluorescence microscope, and images were collected with a cooled CCD camera. Digitally acquired images were processed using the Metamorph software. B, Primary cultures of RPE from mature eyes supplemented with buffer showed a typical microvilli staining pattern for ezrin. C, Moesin expression was diffuse throughout the cytoplasm of the cells with puncta of undefined origin. No changes in the ezrin (D) and moesin (E) labeling were observed when monolayers were supplemented with ezrin sense oligonucleotides. In sharp contrast, monolayers supplemented with antisense oligonucleotides almost completely lost their ezrin staining (F) while their moesin staining (G) did not change significantly from the control samples. Bars, 10 μm.

The immunofluorescence observations were confirmed by both scanning (Fig. 7, A, C, and E) and transmission (Fig. 7, B, D, and F) EM. Untreated primary RPE cultures displayed an apical surface densely covered by microvilli (Fig. 7, A and B) and a basal surface with elaborate basal infoldings (Fig. 7 B). Control monolayers treated with ezrin sense oligonucleotides were essentially unchanged (Fig. 7, C and D). Strikingly, treatment of primary RPE

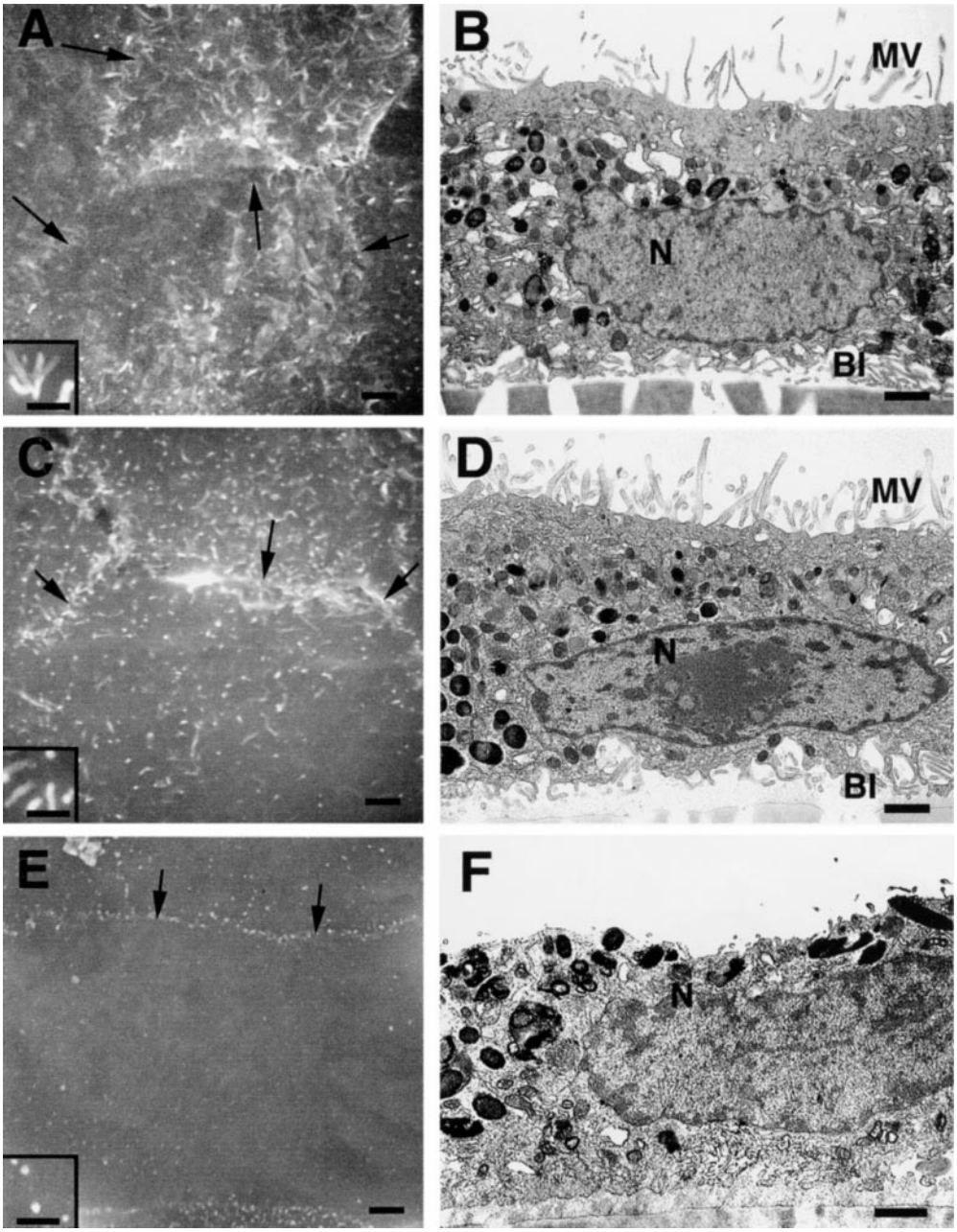

Figure 7. Treatment of primary cultures with ezrin antisense oligonucleotide disrupts apical microvilli and basal infoldings. Scanning and transmission EM. Primary RPE cultures plated on glass coverslips or on filters were treated with 20 μM sense or antisense oligonucleotides directed to ezrin for 96 h as previously described. After treatment, monolayers were fixed in 2.5% glutaraldehyde, sequentially dehydrated, and processed for observation at both scanning (A, C, and E) and transmission (B, D, and F) EM. Untreated primary RPE cultures (A and B) displayed an apical surface densely covered by microvilli and a basal surface with elaborated basal infoldings (B). Strikingly, monolayers treated with ezrin antisense oligonucleotide displayed a smooth surface, almost completely deprived of microvilli (E and F) and basal infoldings (F). On the other hand, monolayers treated with ezrin sense oligonucleotides displayed normal microvilli on their apical surfaces (C and D) and elaborated basal infoldings (D). Insets A, C, and E show that not only the number, but also the length, of microvilli is affected by the treatment of the cultures with ezrin antisense oligonucleotides. Adhesion sites between cells are indicated by the small arrows. BI, basal infoldings; MV, microvilli; N, nuclei. Bars: (A, C, and E) 2 μm; (insets in A, C, and E) 0.5 μm; (B, D and F) 1 μm.

cultures with ezrin antisense oligonucleotides caused almost complete disappearance of microvilli (Fig. 7, E and F) and of basal infoldings (Figs. 7 F). Observation at higher magnification (Fig. 7, insets) demonstrated that microvilli in monolayers treated with antisense oligonucleotides (Fig. 7 E) were very short and sparse (Fig. 7 E), in stark contrast with the long and abundant microvilli of control (Fig. 7 A) and sense oligonucleotide-treated (Fig. 7 C) samples. The data are consistent with a stringent requirement for high levels of ezrin protein and with a limited role of moesin in the maintenance of apical RPE microvilli and basal infoldings.

Ezrin Is Not Bound to the Cortical Cytoskeleton, Whereas Moesin Is Bound to the Basolateral Actin Cytoskeleton of the RPE-J Cell Line

To further analyze the morphogenetic role of ezrin in RPE cells we analyzed ezrin distribution and levels of expression in RPE-J cells, a rat cell line established in our laboratory that preserves many native RPE characteristics (Nabi et al., 1993; Bonilha et al., 1997), including the ability to perform phagocytosis of outer segments (Finnemann et al., 1997). In contrast with primary RPE cultures, RPE-J cells possess sparse and short microvilli at their apical surface and no basal infoldings (Nabi et al., 1993; Marmor-

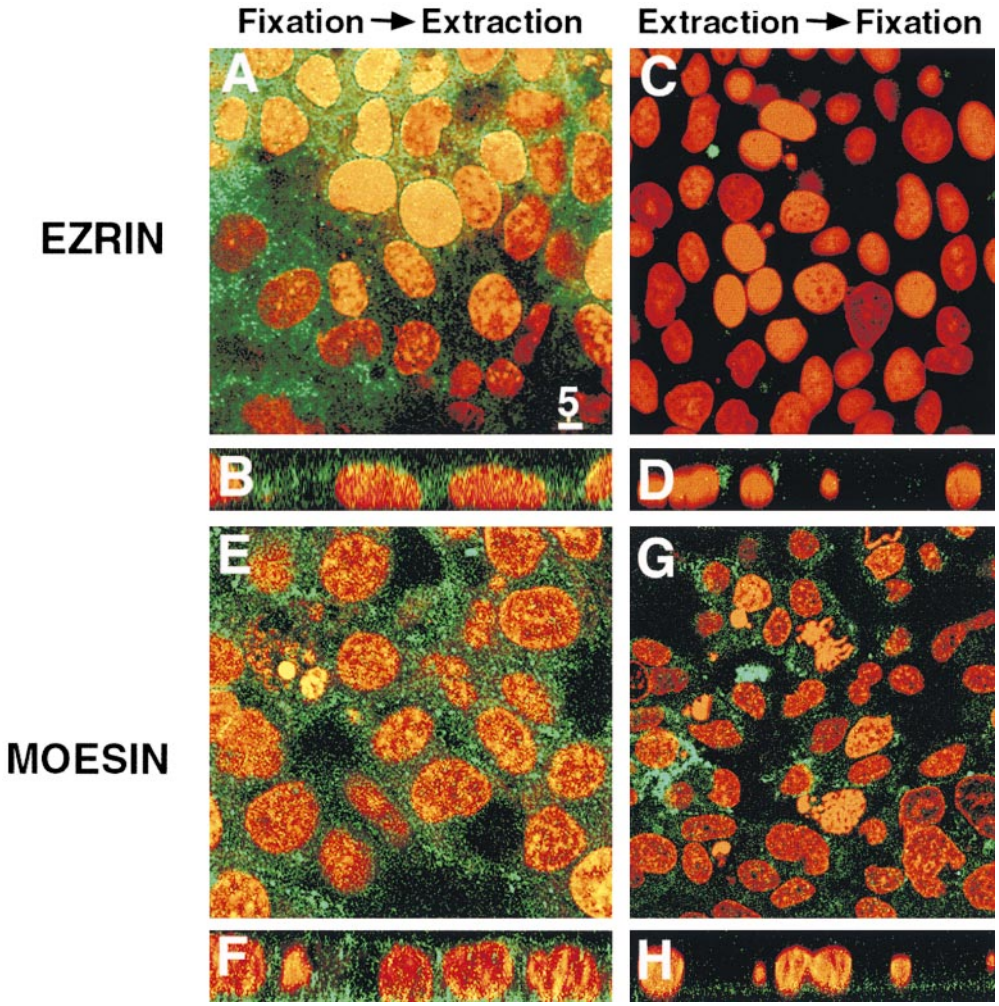

Figure 8. Ezrin is mostly cytoplasmic, whereas moesin is mostly bound to the basolateral surface of RPE-J cells. Polarized RPE-J monolayers were plated on filters, processed as indicated below, and labeled either with an mAb specific to ezrin (A–D) or with a pAb specific to moesin (E–H). RPE-J cells fixed with paraformaldehyde before extraction with Triton X-100 displayed ezrin (A and B) and moesin (E and F) labeling diffusely distributed in the cytoplasm. Most of the ezrin staining was removed when cells were extracted before fixation (C and D). Moesin was detected mostly at the basal surface of cells extracted before fixation, suggesting preferential attachment to the basolateral cytoskeleton of RPE-J cells (G and H). Bar, 5 μm.

stein et al., 1998). Confocal microscopy examination of paraformaldehyde-fixed RPE-J monolayers grown on polycarbonate filters revealed a diffuse cytoplasmic distribution of ezrin (Fig. 8, A and B). Moesin staining appeared to be slightly more granular and also extended throughout the cytoplasm (Fig. 8 E). Examination of cross-sections of these monolayers showed that moesin was evenly distributed over the apical and basolateral surfaces of RPE-J cells (Fig. 8 F). To test whether the diffuse cytoplasmic distribution of ezrin in RPE-J cells reflected a weak or absent interaction of ezrin with the actin cytoskeleton, we carried out standard detergent extractability assays. Extraction of monolayers with 0.5% Triton X-100 and fixation with paraformaldehyde removed most of the ezrin in RPE-J cells (Fig. 8, C and D), suggesting that in these cells, ezrin is not anchored to the actin cytoskeleton. In contrast, a larger fraction of moesin staining was preserved in monolayers treated with detergent and appeared to be concentrated at the base of the cells, below the nuclei (Fig. 8, G and H).

Transfection of Ezrin into RPE-J Cells Promotes the Association of Ezrin with the Cytoskeleton and the Development of Apical Microvilli and Basal Infoldings

To provide additional evidence for the role of ezrin in the assembly of RPE microvilli and basal infoldings, we generated stably transfected RPE-J cells overexpressing human ezrin tagged with a VSVG cytoplasmic epitope (Algrain et al., 1993). Immunoblot experiments indicated that RPE-J cells express no radixin and low levels of ezrin and moesin (ratio 1.15:1), comparable to immature (P2) RPE (Fig. 4) and three to four times lower than primary cultures of adult RPE cells (Fig. 9 A). RPE-J clones 6, 16, and 20 overexpressed VSVG-tagged ezrin at levels two to four times higher than wild-type RPE-J (Fig. 9 A). Interestingly, these RPE-J clones displayed a significantly higher proportion of cytoskeleton-associated ezrin than wild-type RPE-J cells (63 ± 8.6%, 58 ± 3.5%, and 69 ± 6.8%, for clones 6, 16, and 20, compared with 37 ± 2.1% in wild-type RPE-J, as determined by resistance to Triton X-100 extraction; Fig. 9 B). Immunofluorescence experiments of monolayers sequentially extracted and fixed showed that >70% of the cells in these RPE-J clones expressed transfected ezrin and displayed an apical microvilli pattern resistant to detergent extraction (Fig. 9, E, G, and I) that was not observed in control RPE-J cells (Fig. 8, A–D). Importantly, moesin levels were not altered (Fig. 9 A) and its partition into the detergent-resistant fraction was not significantly increased (Fig. 9 B) by ezrin overexpression (53 ± 6.9%, 47 ± 5.6%, and 40 ± 7.3% in clones 6, 16, and 20, respectively, compared with 57 ± 3.8% in control RPE-J

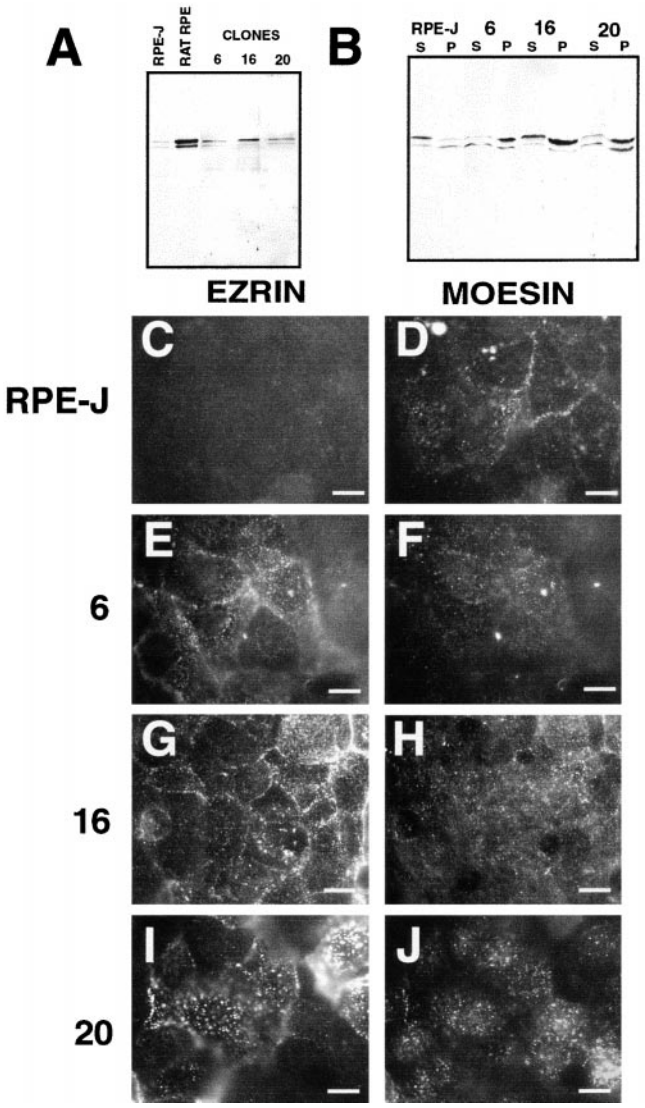

Figure 9. Overexpression of ezrin in RPE-J cells promotes its localization into detergent-resistant apical microvilli. A, 10 μg of whole cell lysates of RPE-J and primary cultures were loaded into 7.5% SDS-PAGE gels, and resolved proteins were transferred to nitrocellulose membranes, followed by immunoblot with a pAb to a peptide conserved in all three ERM proteins. Values shown are the mean of four independent experiments. Ezrin levels in wild-type RPE-J cells (RPE-J) were three times lower than in primary RPE cells (RAT RPE); ezrin:moesin ratio was 1.15:1 in RPE-J and 1.7 in primary RPE cultures. RPE-J clones overexpressing ezrin showed two times (clone 6) or three to four times (clones 16 and 20) higher total ezrin expression levels than wild-type RPE-J cells (RPE-J). B, RPE clones overexpressing ezrin displayed larger pools of ezrin associated with the cytoskeleton. In wild-type RPE-J cells (RPE-J, P), 37 ± 2.1% of ezrin and 57 ± 3.8% of moesin was resistant to extraction by Triton X-100. In RPE-J clones (6, 16, and 20, P), the cytoskeleton-associated fraction of ezrin was increased to 63 ± 8.6%, 58 ± 3.5%, and 69 ± 6.8% for clones 6, 16, and 20, respectively. Moesin partition into the detergent-resistant fraction was 53 ± 6.9%, 47 ± 5.6%, and 40 ± 7.3%, for clones 6, 16, and 20, respectively. 20–30 μg and ~60–80 μg of the detergent soluble and insoluble fractions were loaded per lane. C–J, Immunofluorescence of RPE-J clones overexpressing ezrin. Wild-type RPE-J cells (C and D) and RPE-J clones overexpressing ezrin (E–J) were extracted with Triton X-100, fixed, and stained with an antibody against a VSVG epitope (C, E, G, and I) and an antibody against moesin (D, F, H, and J). Control RPE-J cells showed a low background staining with the VSVG epitope antibody (C). All three RPE-J clones overexpressing ezrin displayed a strong and homogeneous apical microvilli pattern that was resistant to detergent extraction (E, G, and I). Detergent-resistant moesin in RPE-J cells had a basolateral distribution (D), but acquired a more diffuse distribution and was present in puncta of undefined origin in RPE-J clones (F, H, and J). Bar, 10 μm.

cells). Overexpression of ezrin appeared to promote a subtle change in moesin distribution, from a preferentially basolateral distribution (Fig. 9 D) to a more diffuse cytoplasmic staining (Fig. 9, F, H, and J).

The ultrastructure of RPE-J clones overexpressing the human ezrin cDNA was analyzed by scanning (Fig. 10, A, C, and E) and transmission (Fig. 10, B, D, and F) EM. As previously shown (Nabi et al., 1993), RPE-J cells display very short and scattered microvilli at their apical surface (Fig. 10, A and B) and no basal infoldings (Fig. 10 B). Fig. 10 shows electronmicrographs of clones 6 (Fig. 10, C and D) and 20 (Fig. 10, E and F). RPE-J cells transfected with ezrin exhibited an increase in the number and length of their apical microvilli (Fig. 10, C and E, see corresponding insets). Fig. 10 D illustrates the presence of basal infoldings in clone 6. Taken together, the data presented in this section demonstrate that overexpression of ezrin in RPE-J cells is sufficient to induce both apical microvilli and basal infoldings.

Discussion

The results of the experiments in this report provide strong evidence for a specific morphogenetic role of ezrin in RPE. Moesin appears not to be required for these morphogenetic events, as it is not expressed by RPE in vivo, and is largely not affected by the two in vitro strategies employed. The third member of the ERM family, radixin, was not detected in either RPE in situ or under culture conditions, indicating that, as is the case with moesin, it is not normally involved in these processes.

The first important evidence in support of a specific morphogenetic role of ezrin was provided by immunolocalization studies in rat eyes. Colloidal gold immunoelectron microscopy decorated ezrin along the entire actin filamentous core of RPE microvilli and throughout the convoluted basal infoldings (Fig. 3). The data extend prior observations that demonstrated the presence of ezrin in RPE microvilli (Hofer and Drenckhahn, 1993). As in most other epithelia (Berryman et al., 1993), ezrin was accompanied by no other ERM protein. Only a few epithelial tissues display ezrin and moesin in microvilli and, in just one case (the hepatic bile canaliculi), moesin is the only ERM protein expressed in epithelial microvilli (Berryman et al., 1993). On the other hand, moesin, but not ezrin, is expressed in endothelial cells. A basolateral localization of ezrin has previously been reported for immature enterocytes in intestinal crypts, for the intricate podocyte extensions to the glomerular basement membrane in renal corpuscles (Berryman et al., 1993), and for the basolateral membrane infoldings of both resting and stimulated pari-

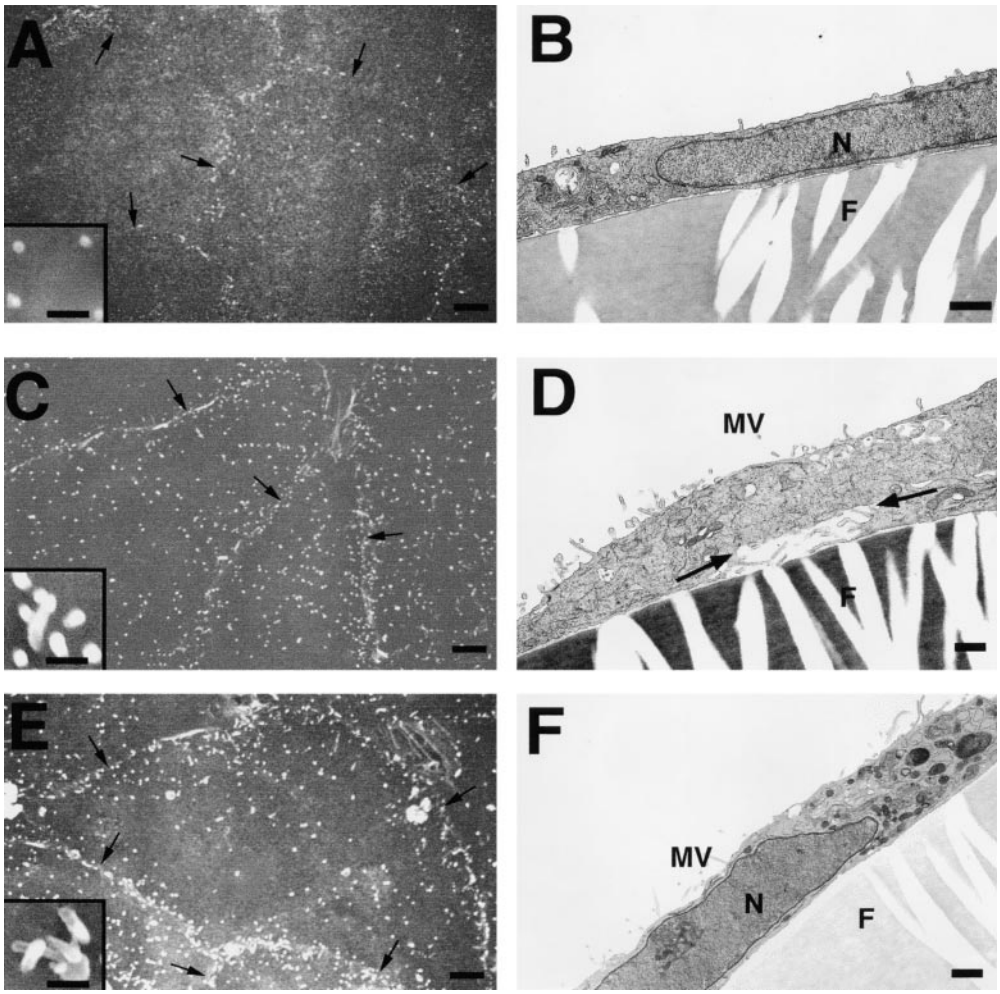

Figure 10. RPE-J clones overexpressing ezrin develop apical microvilli-like structures and basal infoldings. The ultrastructure of RPE-J cells overexpressing ezrin was analyzed by transmission EM. Polarized monolayers plated on glass coverslips or on filters were fixed in 2.5% glutaraldehyde, sequentially dehydrated, and observed both by scanning (A, C, and E) and transmission (B, D, and F) EM. Untransfected RPE-J cells showed scattered stubby microvilli at their apical surface (A and B) and a smooth basal surface (B). Clones 6 and 20, overexpressing ezrin, developed numerous apical microvilli-like structures (C–F) and some basal infoldings (D, arrows). Insets in A, C, and E show that not only the number, but also the length, of microvilli is affected by the overexpression of exogenous ezrin in RPE-J cultures. Adhesion sites between cells are indicated by the small arrows. F, filter; MV, microvilli; N, nucleus. Bars: (A, C and E) 2 μm; (insets in A, C, and E) 0.5 μm; (B, D, and F) 1 μm.

etal cells (Hanzel et al., 1991). The localization of ezrin at apical and basolateral membranes of RPE cells is likely to depend on the interaction with different plasma membrane proteins. In fact, studies carried out in parietal cells showed that ezrin can bind to proteins that are localized either apically or basolaterally (Hanzel et al., 1991; Yao et al., 1993, 1996). Experiments in other cell systems have identified several plasma membrane proteins that bind the NH_2-terminal domain of ezrin, including CD44, CD43, proton transporting ATPase, ICAM-1, ICAM-2, and peripheral membrane proteins (such as EBP50) that may act as a bridge between ezrin and the plasma membrane. It is not known at present which RPE proteins anchor ezrin to the apical or to the basal plasma membrane of RPE.

A second important piece of evidence for a role of ezrin in RPE morphogenesis was provided by developmental studies that showed a direct correlation between spacial and temporal increase in ezrin expression and the development of surface differentiations of RPE. Immunoblots of whole RPE cell lysates at different days after birth demonstrated that the ezrin levels increased fourfold as the RPE developed microvilli and basal infoldings and established adult interactions with PRs and the basement membrane. This correlates well with the reported fourfold increase in actin content during maturation of chicken RPE (in chicken, as in humans, the maturation of the retina occurs before birth; Owaribe and Eguchi, 1985), which reflects the structural need for these two proteins in the assembly of microvilli and basal infoldings. As immunoblots of RPE lysates obtained from rats of different ages did not detect the presence of moesin or radixin (Fig. 4), we can discard a possible additional role of these proteins in vivo. Ezrin has been identified as a minor component of apical brush borders of intestinal and renal epithelial cells and a previous report described an increase in ezrin mRNA as intestinal cells matured from an embryonic stage to a mature morphologically differentiated stage (Barila et al., 1995). However, in intestinal and kidney epithelia, potential morphogenetic roles of ezrin and other ERM proteins are overshadowed by the contribution of villin, a major component of microvilli that is a major player in the assembly of these structures.

A third piece of evidence in support of a morphogenetic role of ezrin was provided by antisense oligonucleotide experiments. We speculated that, since villin is not expressed by RPE (Hofer and Drenckhahn, 1993), the possible contributions of ezrin might be relatively more important and easier to detect in this model system. Experiments in which ezrin antisense oligonucleotides were added to primary cultures of mature RPE cells, which preserve apical microvilli and basal infoldings (Stramm et al., 1983; Heth et al., 1987; Gundersen et al., 1993; Davis et al., 1995),

yielded a striking result: 80% drop in ezrin levels resulted in a striking decrease in the number and length of RPE microvilli and the complete disappearance of basal infoldings. Our studies markedly differ from two previous reports in which an antisense approach was used to explore the function of ERM proteins. In the experiments by Takeuchi et al. (1994) and Paglini et al. (1998), a mixture of antisense nucleotides against two to three ERM proteins was required to observe a clear morphogenetic effect on, respectively, microvilli or growth cone extension; in our experiments with RPE cells, antisense oligonucleotides against just ezrin cause a dramatic morphological effect. Ezrin antisense oligonucleotides did not affect, or decreased only marginally, moesin expression. Furthermore, since moesin was preferentially associated with the basolateral membrane, the data does not support an important role of this protein in the development and maintenance of RPE microvilli. In addition, since moesin was not detected in RPE in vivo, it is obviously not involved in the morphogenesis of basolateral infoldings in vivo, although it might contribute to their formation in vitro.

A fourth important piece of evidence for a role of ezrin in RPE morphogenesis was provided by transfection and overexpression of ezrin cDNA into cultures of the rat RPE cell line, RPE-J. Although this cell line preserves many native RPE functions, such as similar targeting and sorting of some plasma membrane proteins and the phagocytosis of PR outer segments (Nabi et al., 1993; Bonilha et al., 1997; Finnemann et al., 1997; Marmorstein et al., 1998), it does not preserve the characteristic apical microvilli and basal infoldings of RPE in situ. In contrast with primary RPE cultures, which displayed high levels of insoluble ezrin preferentially associated with the apical microvilli, RPE-J cells had three- to fourfold lower ezrin levels, a diffuse cytoplasmic distribution, and a larger proportion of detergent-soluble ezrin, indicative of a poor association with the actin cytoskeleton. As in primary RPE cultures, moesin was preferentially associated to the basolateral cytoskeleton of RPE-J cells. Because the data suggested that higher levels of expression of ezrin associated with the cytoskeleton is an important factor in the establishment of apical microvilli and basal infoldings in RPE, we studied the effect of stable ezrin overexpression by transfection into RPE-J cells. Analysis of clones with different levels of ezrin expression detected a clear correlation between high levels of ezrin expression and the formation of apical microvilli and basal infoldings. Furthermore, overexpressed ezrin showed an increased resistance to detergent extraction and microvillar localization.

Our transfection data contrast with previous studies in which ezrin overexpression failed to observe any striking modification of cell surface morphology. Transfection of full-length ezrin cDNA into monkey kidney cells resulted in the accumulation of ezrin underneath the plasma membrane in actin-containing membrane protrusions, such as microspikes, filopodia, and microvilli, with no obvious reorganization of actin-containing structures (Algrain et al., 1993). Microinjection of ezrin protein into living gastric cells resulted in the accumulation of the protein at microvilli and other membrane locations without inducing morphological changes (Andreoli et al., 1994). On the other hand, overexpression of the COOH-terminal domains of ezrin and radixin, which bind to F-actin, induced clear surface alterations (Henry et al., 1995; Martin et al., 1995, 1997), whereas overexpression of the NH_2-terminal domain of ezrin and moesin reduced the size and number of microvilli in LLC-PK cells (Algrain et al., 1993; Crepaldi et al., 1997) and interfered with surface structures of fibroblasts (Amieva et al., 1998). The lack of effect of transfected full size ezrin in some cell systems may reflect its inactivated monomer state, and the absence of cellular activating mechanisms. Our transfection experiments suggest that RPE-J cells retain some capacity to activate ezrin into the assembly of microvilli. However, as the induced microvilli are relatively short compared with those present in native adult RPE, additional factors needed for the assembly of RPE microvilli may be in short supply in RPE-J cells or the balance of ezrin activation and deactivation systems may not be the same as in native RPE. As RPE-J cells express lower ezrin levels than primary RPE cultures and many other cell lines, ezrin expression in RPE-J cells may be below the threshold necessary to ensure cell spreading and morphological changes driven by exchanges between the soluble and membrane–cytoskeleton-associated pools.

The results of this report suggest that moesin expression cannot substitute for ezrin in the generation of apical microvilli and basal infoldings in RPE cells, thus supporting a very specific role of ezrin in these processes. Our results suggest that RPE cells express specific ezrin binding proteins in the apical surface which cannot bind moesin as efficiently. Moesin, on the other hand, may bind other plasma membrane proteins which are not essential in the establishment or maintenance of RPE microvilli or basal infoldings. It is quite clear that ERM proteins bind specific motifs in plasma membrane proteins and that this binding is essential for their morphogenetic effects (Yonemura et al., 1999). The apparent specificity of ERM protein function supported by our data apparently conflicts with the observation that moesin knockout mice fail to show obvious histological abnormalities, or deficiencies in various cellular processes previously attributed to moesin, which implies functional redundancy of ERM proteins at both cellular and whole body level (Doi et al., 1999). Since this study excluded the eye, future experiments in which ezrin expression in the eye is blocked in vivo should help provide an answer to this paradox.

The dramatic changes in ezrin expression during developmental maturation and the striking effects of ezrin antisense and overexpression turn RPE into an excellent model to study in detail the function of ezrin and the associated proteins in vivo and in vitro. The uniqueness of the RPE system may lie in the special complement of cytoskeletal proteins expressed by these cells. Our results with both the suppression of ezrin expression in primary cultures and the overexpression of ezrin in RPE-J cells are very similar to previous reports about villin function in the generation of brush border microvilli (Friederich et al., 1989; Costa de Beauregard et al., 1995). However, whereas villin participates in the Ca^{2+}-dependent bundling of actin filaments, there is no evidence that ezrin could perform a similar role, even in a Ca^{2+}-independent manner. In this regard, ezrin interaction with actin filaments may be much more complex than originally imagined. Recent work has

indicated that ezrin has the ability to stimulate actin polymerization and preferentially bind to nonmuscle β-actin isoforms in vitro (Yao et al., 1996). Furthermore, an actin binding site which mediates binding to both G-actin, as well as to F-actin, has been mapped to ezrin residues 281–310 (Roy et al., 1997) and the sequence between amino acids 558–578 of ezrin, radixin, and moesin is highly homologous to the actin binding site of the barbed-end capping protein CapZ β subunit (Turunen et al., 1994). Taken together, these data suggest that ezrin and the other ERM proteins may also have barbed-end capping activity in vivo, thus regulating the length of actin filaments by both stimulating and inhibiting actin polymerization. Ongoing work in our laboratory aims to elucidate the molecular components and signaling pathways that regulate ezrin function in RPE cells.

The authors are grateful to Dr. Monique Arpin (Institut Curie, Paris, France) for providing us with the pAb against ezrin and the human VSVG-tagged ezrin cDNA, and to Drs. Anthony Bretscher (Cornell University, Ithaca, NY) and Frank Solomon (Massachusetts Institute of Technology, Cambridge, MA) for their kind gifts of antibodies against moesin and radixin. We thank Leona Cohen-Gould and Dena Almeida for excellent assistance with the EM and cryosectioning of rat eyes.

This work was supported by the National Institutes of Health grant EY08538, and a Jules and Doris Stein professorship from the Research to Prevent Blindness Foundation to E. Rodriguez-Boulan, and a Norman and Rosita Winston Fellowship in Biomedical Research to S.C. Finnemann.

Submitted: 11 May 1999
Revised: 17 November 1999
Accepted: 19 November 1999

References

Algrain, M., O. Turunen, A. Vaheri, D. Louvard, and M. Arpin. 1993. Ezrin contains cytoskeleton and membrane binding domains accounting for its proposed role as a membrane–cytoskeletal linker. *J. Cell Biol.* 120:129–139.

Amieva, M.R., P. Litman, L. Huang, E. Ichimaru, and H. Furthmayr. 1998. Disruption of dynamic cell surface architecture of NIH3T3 fibroblasts by the N-terminal domains of moesin and ezrin: in vivo imaging with GFP fusion proteins. *J. Cell Sci.* 112:111–125.

Andreoli, C., M. Martin, R. Le Borgne, H. Reggio, and P. Mangeat. 1994. Ezrin has properties to self-associate at the plasma membrane. *J. Cell Sci.* 107: 2509–2521.

Arpin, M., M. Algrain, and D. Louvard. 1994. Membrane-actin microfilament connections: an increasing diversity of players related to band 4.1. *Curr. Opin. Cell Biol.* 6:136–141.

Barila, D., C. Murgia, F. Nobili, and G. Perozzi. 1995. Transcriptional regulation of the ezrin gene during rat intestinal development and epithelial differentiation. *Biochim. Biophys. Acta.* 1263:133–140.

Berryman, M., Z. Franck, and A. Bretscher. 1993. Ezrin is concentrated in the apical microvilli of a wide variety of epithelial cells whereas moesin is found primarily in endothelial cells. *J. Cell Sci.* 105:1025–1043.

Bok, D. 1993. The retinal pigment epithelium, a versatile partner in vision. *J. Cell Sci.* 17:189–195.

Bonilha, V.L., A.D. Marmorstein, L. Cohen-Gould, and E. Rodriguez-Boulan. 1997. Apical sorting of hemagluttinin by transcytosis in retinal pigment epithelium. *J. Cell Sci.* 110:1717–1727.

Braekevelt, C.R., and M.J. Hollenberg. 1970. Development of the retinal pigment epithelium, choriocapillaris and Bruch's membrane in the albino rat. *Exp. Eye Res.* 9:124–131.

Bretscher, A. 1983. Purification of an 80,000-dalton protein that is a component of the isolated microvillus cytoskeleton, and its localization in nonmuscle cells. *J. Cell Biol.* 97:425–432.

Bretscher, A. 1989. Rapid phosphorylation and reorganization of ezrin and spectrin accompany morphological changes induced in A-431 cells by epidermal growth factor. *J. Cell Biol.* 108:921–930.

Bretscher, A. 1999. Regulation of cortical structure by the ezrin–radixin–moesin protein family. *Curr. Opin. Cell Biol.* 11:109–116.

Chen, C.A., and H. Okayama. 1988. Calcium phosphate-mediated gene transfer: a highly efficient transfection system for stably transforming cells with plasmid DNA. *Biotechniques.* 6:632–638.

Chishti, A.H., A.C. Kim, S.M. Marfatia, M. Lutchman, M. Hanspal, H. Jindal, S.C. Liu, P.S. Low, G.A. Rouleau, N. Mohandas, et al. 1998. The FERM domain: a unique module involved in the linkage of cytoplasmic proteins to the membrane. *Trends Biochem. Sci.* 23:281–282.

Costa de Beauregard, M.A., E. Pringault, S. Robine, and D. Louvard. 1995. Suppression of villin expression by antisense RNA impairs brush border assembly in polarized epithelial intestinal cells. *EMBO (Eur. Mol. Biol. Organ.) J.* 14:409–421.

Crepaldi, T., A. Gautreau, P.M. Comoglio, D. Louvard, and M. Arpin. 1997. Ezrin is an effector of hepatocyte growth factor-mediated migration and morphogenesis in epithelial cells. *J. Cell Biol.* 138:423–434.

Davis, A.A., P.S. Bernstein, D. Bok, J. Turner, M. Nachtigal, and R.C. Hunt. 1995. A human retinal pigment epithelial cell line that retains epithelial characteristics after prolonged culture. *Invest. Ophthalmol. Vis. Sci.* 36:955–964.

Doi, Y., M. Itoh, S. Yonemura, S. Ishihara, H. Takano, T. Noda, Sh. Tsukita, and Sa. Tsukita. 1999. Normal development of mice and unimpaired cell adhesion/cell motility/actin-based cytoskeleton without compensatory up-regulation of ezrin or radixin in moesin gene knockout. *J. Biol. Chem.* 274: 2315–2321.

Dransfield, D.T., A.J. Bradford, J. Smith, M. Martin, C. Roy, P.H. Mangeat, and J.R. Goldenring. 1997. Ezrin is a cyclic AMP-dependent protein kinase anchoring protein. *EMBO (Eur. Mol. Biol. Organ.) J.* 16:35–43.

Drenckhahn, D., and H.J. Wagner. 1985. Relation of retinomotor responses and contractile proteins in vertebrate retinas. *Eur. J. Cell Biol.* 37:156–168.

Finnemann, S.C., V.L. Bonilha, A.D. Marmorstein, and E. Rodriguez-Boulan. 1997. Phagocytosis of rod outer segments by retinal pigment epithelial cells requires αvβ5 integrin for binding but not for internalization. *Proc. Natl. Acad. Sci. USA.* 94:12932–12937.

Friederich, E., C. Huet, M. Arpin, and D. Louvard. 1989. Villin induces microvilli growth and actin redistribution in transfected fibroblasts. *Cell.* 59: 461–475.

Funayama, N., A. Nagafuchi, N. Sato, Sh. Tsukita, and Sa. Tsukita. 1991. Radixin is a novel member of the band 4.1 family. *J. Cell Biol.* 115:1039–1048.

Girault, J.A., G. Labesse, J.P. Mornon, and I. Callebaut. 1998. Janus kinases and focal adhesion kinases play in the 4.1 band: A superfamily of band 4.1 domains important for cell structure and signal transduction. *Mol. Med.* 4:751–769.

Gundersen, D., S.K. Powell, and E. Rodriguez-Boulan. 1993. Apical polarization of N-CAM in retinal pigment epithelium is dependent on contact with the neural retina. *J. Cell Biol.* 121:335–343.

Hanzel, D., H. Reggio, A. Bretscher, J.G. Forte, and P. Mangeat. 1991. The secretion-stimulated 80K phosphoprotein of parietal cells is ezrin, and has properties of a membrane cytoskeletal linker in the induced apical microvilli. *EMBO (Eur. Mol. Biol. Organ.) J.* 10:2363–2373. [published erratum appears in *EMBO (Eur. Mol. Biol. Organ.) J.* 1991. 10:3978–3981].

Hasson, T., and M.S. Mooseker. 1995. Molecular motors, membrane movements and physiology: emerging roles for myosins. *Curr. Opin. Cell Biol.* 7:587–594.

Henry, M.D., C. Gonzalez Agosti, and F. Solomon. 1995. Molecular dissection of radixin: distinct and interdependent functions of the amino- and carboxy-terminal domains. *J. Cell Biol.* 129:1007–1022.

Heth, C.A., M.A. Yankauckas, M. Adamian, and R.B. Edwards. 1987. Characterization of retinal pigment epithelial cells cultured on microporous filters. *Curr. Eye Res.* 6:1007–1019.

Hirao, M., N. Sato, T. Kondo, S. Yonemura, M. Monden, T. Sasaki, Y. Takai, Sh. Tsukita, and Sa. Tsukita. 1996. Regulation mechanism of ERM (ezrin/radixin/moesin) protein/plasma membrane association: possible involvement of phosphatidylinositol turnover and Rho-dependent signaling pathway. *J. Cell Biol.* 135:37–51.

Hofer, D., and D. Drenckhahn. 1993. Molecular heterogeneity of the actin filament cytoskeleton associated with microvilli of photoreceptors, muller glial cells and pigment epithelial cells of the retina. *Histochemistry.* 99:29–35.

Kreis, T.E. 1986. Microinjected antibodies against the cytoplasmic domain of vesicular stomatitis virus glycoprotein block its transport to the cell surface. *EMBO (Eur. Mol. Biol. Organ.) J.* 5:931–941.

Kreis, T.E. 1987. Microtubules containing detyrosinated tubulin are less dynamic. *EMBO (Eur. Mol. Biol. Organ.) J.* 6:2597–2606.

Lamb, R.F., B.W. Ozanne, C. Roy, L. McGarry, C. Stipp, P. Mangeat, and D.G. Jay. 1997. Essential functions of ezrin in maintenance of cell shape and lamellipodial extension in normal and transformed fibroblasts. *Curr. Biol.* 7:682–688.

Lankes, W.T., and H. Furthmayr. 1991. Moesin: a member of the protein 4.1-talin–ezrin family of proteins. *Proc. Natl. Acad. Sci. USA.* 88:8297–8301.

Liu, X., G. Vansant, I.P. Udovichenko, U. Wolfrum, and D.S. Williams. 1997. Myosin VIIa, the product of the Usher 1B syndrome gene, is concentrated in the connecting cilia of photoreceptor cells. *Cell Motil. Cytoskelet.* 37:240–252.

Mangeat, P., C. Roy, and M. Martin. 1999. ERM proteins in cell adhesion and membrane dynamics. *Trends Cell Biol.* 9:187–192.

Marmorstein, A.D., Y.C. Gan, V.L. Bonilha, S.C. Finnemann, K.G. Csaky, and E. Rodriguez-Boulan. 1998. Apical polarity of N-CAM and EMMPRIN in retinal pigment epithelium resulting from suppression of basolateral signal recognition. *J. Cell Biol.* 142:697–710.

Martin, M., C. Andreoli, A. Sahuquet, P. Montcourrier, M. Algrain, and P. Mangeat. 1995. Ezrin NH_2-terminal domain inhibits the cell extension activity of the COOH-terminal domain. *J. Cell Biol.* 128:1081–1093.

Martin, M., C. Roy, P. Montcourrier, A. Sahuquet, and P. Mangeat. 1997.

Three determinants in ezrin are responsible for cell extension activity. *Mol. Biol. Cell*. 8:1543–1557.

Matsui, T., M. Maeda, Y. Doi, S. Yonemura, M. Amano, K. Kaibuchi, Sa. Tsukita, and Sh. Tsukita. 1998. Rho-kinase phosphorylates COOH-terminal threonines of ezrin/radixin/moesin (ERM) proteins and regulates their head-to-tail association. *J. Cell Biol*. 140:647–657.

Nabi, I.R., A.P. Mathews, L. Cohen-Gould, D. Gundersen, and E. Rodriguez-Boulan. 1993. Immortalization of polarized rat retinal pigment epithelium. *J. Cell Sci*. 104:37–49.

Owaribe, K., and G. Eguchi. 1985. Increase in actin contents and elongation of apical projections in retinal pigmented epithelial cells during development of the chicken eye. *J. Cell Biol*. 101:590–596.

Paglini, G., P. Kunda, S. Quiroga, K. Kosik, and A. Caceres. 1998. Suppression of radixin and moesin alters growth cone morphology, motility, and process formation in primary cultured neurons. *J. Cell Biol*. 143:443–455.

Pestonjamasp, K., M.R. Amieva, C.P. Strassel, W.M. Nauseef, H. Furthmayr, and E.J. Luna. 1995. Moesin, ezrin, and p205 are actin-binding proteins associated with neutrophil plasma membranes. *Mol. Biol. Cell*. 6:247–259.

Pietromonaco, S.F., P.C. Simons, A. Altman, and L. Elias. 1998. Protein kinase C-theta phosphorylation of moesin in the actin-binding sequence. *J. Biol. Chem*. 273:7594–7603.

Reczek, D., M. Berryman, and A. Bretscher. 1997. Identification of EBP50: A PDZ-containing phosphoprotein that associates with members of the ezrin–radixin–moesin family. *J. Cell Biol*. 139:169–179.

Roy, C., M. Martin, and P. Mangeat. 1997. A dual involvement of the amino-terminal domain of ezrin in F- and G-actin binding. *J. Biol. Chem*. 272: 20088–20095.

Schwartz-Albiez, R., A. Merling, H. Spring, P. Moller, and K. Koretz. 1995. Differential expression of the microspike-associated protein moesin in human tissues. *Eur. J. Cell Biol*. 67:189–198.

Shaw, R.J., M. Henry, F. Solomon, and T. Jacks. 1998. RhoA-dependent phosphorylation and relocalization of ERM proteins into apical membrane/actin protrusions in fibroblasts. *Mol. Biol. Cell*. 9:403–419.

Simons, P.C., S.F. Pietromonaco, D. Reczek, A. Bretscher, and L. Elias. 1998. C-terminal threonine phosphorylation activates ERM proteins to link the cell's cortical lipid bilayer to the cytoskeleton. *Biochem. Biophys. Res. Commun*. 253:561–565.

Stramm, L.E., M.E. Haskins, M.M. McGovern, and G.D. Aguirre. 1983. Tissue culture of cat retinal pigment epithelium. *Exp. Eye Res*. 36:91–101.

Takahashi, K., T. Sasaki, A. Mammoto, K. Takaishi, T. Kameyama, Sa. Tsukita, Sh. Tsukita, and Y. Takai. 1997. Direct interaction of the Rho GDP dissociation inhibitor with ezrin/radixin/moesin initiates the activation of the Rho small G protein. *J. Biol. Chem*. 272:23371–23375.

Takeuchi, K., N. Sato, H. Kasahara, N. Funayama, A. Nagafuchi, S. Yonemura, Sa. Tsukita, and Sh. Tsukita. 1994. Perturbation of cell adhesion and microvilli formation by antisense oligonucleotides to ERM family members. *J. Cell Biol*. 125:1371–1384.

Tsukita, Sa., Y. Hieda, and Sh. Tsukita. 1989a. A new 82-kD barbed end-capping protein (radixin) localized in the cell-to-cell adherens junction: purification and characterization. *J. Cell Biol*. 108:2369–2382.

Tsukita, Sa., K. Oishi, N. Sato, J. Sagara, and A. Kawai. 1994. ERM family members as molecular linkers between the cell surface glycoprotein CD44 and actin-based cytoskeletons. *J. Cell Biol*. 126:391–401.

Tsukita, Sh., M. Itoh, and Sa. Tsukita. 1989b. A new 400-kD protein from isolated adherens junction: its localization at the undercoat of adherens junctions and at microfilament bundles such as stress fibers and circumferential bundles. *J. Cell Biol*. 109:2905–2915.

Turunen, O., T. Wahlstrom, and A. Vaheri. 1994. Ezrin has a COOH-terminal actin-binding site that is conserved in the ezrin protein family. *J. Cell Biol*. 126:1445–1453.

Vaughan, D.K., and S.K. Fisher. 1987. The distribution of F-actin in cells isolated from vertebrate retinas. *Exp. Eye Res*. 44:393–406.

Yao, X., A. Thibodeau, and J.G. Forte. 1993. Ezrin-calpain I interactions in gastric parietal cells. *Am. J. Physiol*. 265:C36–C46.

Yao, X., L. Cheng, and J.G. Forte. 1996. Biochemical characterization of ezrin-actin interaction. *J. Biol. Chem*. 271:7224–7229.

Yonemura, S., Sa. Tsukita, and Sh. Tsukita. 1999. Direct involvement of ezrin/radixin/moesin (ERM)-binding membrane proteins in the organization of microvilli in collaboration with activated ERM proteins. *J. Cell Biol*. 145: 1497–1509.

Zinn, K.M., and J.V. Benjamin-Henkind. 1979. Anatomy of the human retinal pigment epithelium. *In* The Retinal Pigment Epithelium. K.M. Zinn and M.F. Marmor, editors. Harvard University Press, Cambridge, MA. 3–31.